Available online at www.sciencedirect.com

ScienceDirect

Procedia Engineering 81 (2014) 1300 – 1305

Procedia Engineering

www.elsevier.com/locate/procedia

11th International Conference on Technology of Plasticity, ICTP 2014, 19-24 October 2014, Nagoya Congress Center, Nagoya, Japan

Numerical simulation of the mechanical response during strain path change: application to Zn alloys

Marina Borodachenkova[a],Wei Wen[a,]*, Frédéric Barlat[a,b], António Pereira[a], José Grácio[a]

[a]*Center for Mechanical Technology and Automation, Mechanical Engineering Department, University of Aveiro, 3810 Aveiro, Portugal*
[b]*Graduate Institute of Ferrous Technology (GIFT), Pohang University of Science and Technology (POSTECH), 77 cheongam-ro, Nam-gu, Pohang, Gyeongbuk 790-784, Korea.*

Abstract

The microstructure-based hardening model (Beyerlein and Tomé, 2007), that accounts for the dislocation reversal-related mechanisms and the cut-through effect, is extended to HCP metals. This model, which is embedded in the visco-plastic self-consistent framework, is applied in this work to predict the mechanical response of Zn alloy during strain path change. The predicted mechanical behavior and texture evolution during pre-loading and reloading is in good agreement with experimental observations. The change in hardening behavior after reloading is well reproduced by this model. The contributions of the different mechanisms are also analyzed.

Selection and peer-review under responsibility of the Department of Materials Science and Engineering, Nagoya University

Keywords: Hardening behavior; Strain path change; Bauschinger effect; Visco-plastic self-consistent model; Zn alloys

1. Introduction

Modeling of the plastic response of a material after a strain path change, particularly after a large prestrain, for which texture and microstructure evolutions introduce strong anisotropy, is a complex task. It requires the consideration of the additional mechanisms activated during the change of the loading direction. In order to describe the hardening evolution of metallic material during deformation processes, microstructure-based hardening laws are usually embedded in the framework of crystal plasticity models.

* Corresponding author. Tel.: +351-234-370-827; fax: +351-234-370-953.
E-mail address: wwen@ua.pt

Selection and peer-review under responsibility of the Department of Materials Science and Engineering, Nagoya University
doi:10.1016/j.proeng.2014.10.147

The Voce law, one of the classic strain hardening models, has been used in many investigations (e.g. Agnew and Duygulu, 2005, Agnew et al., 2001, Proust et al., 2009; Wang et al., 2013). However, this law is not able to correctly predict the mechanical behavior of metals during a strain path change process due to the lack of microstructure description (Beyerlein and Tomé, 2007). In order to capture the flow stress response when the strain path changes, Beyerlein and Tomé (2007) proposed a hardening model based on the Voce law. This model enables the measurement of the directionality and magnitude of previous and current shear for each slip plane in each grain. New formulations are proposed to consider the effect of dislocation-related mechanisms as correction terms to the critical resolved shear stress (CRSS) calculated by the Voce law. This model has been implemented in the VPSC model (Molinari et al., 1987; Lebensohn and Tomé, 1993) and utilized to predict the flow stress response of pure polycrystalline copper subjected to the tension-compression test (Beyerlein and Tomé, 2007).

The goal of the present work is to investigate the influence of reverse loading on the mechanical behavior of a zinc alloy sheet at room temperature. Forward and reverse simple-shear test are conducted on the rolled Zinc alloy sheet to determine the flow curve. In addition, the pole figures are measured at different stages of the deformation process. The mechanical response and texture evolution predicted by the Beyerlein and Tomé (2007) hardening model.

2. Experimental details

Flat rectangular zinc alloy sheet specimens (50 mm long, 15 mm wide and 1 mm thick) were deformed under the simple shear test procedure, which was developed by Rauch (1998). The samples were machined from the rolled Zn alloy sheet with the longitudinal axis in the rolling direction. Specimens were mounted in the shear device installed on a standard tension-compression machine and clamped between two grips, one fixed and the other translating. Simple shear deformation occurs in the 3 mm wide zone between the grips. Monotonic loading was conducted up to a shear strain of 70%. In addition, 20% shear prestrain followed by a load reversal, obtained by changing the direction of the moving grip, was performed up to a shear strain of 60%.

Pole figure measurements were carried out on an X-ray texture goniometer. The pole figures of the initial texture are shown in Fig. 1. The surface texture of the rolled sheet is characterized by a 20^{o} c-axis tilt from the normal direction to rolling direction. The textures after 20% prestrain and after 60% reverse shear are also analyzed. From the processed data of the initial texture, a discrete set of 2122 grains were weighted, extracted and used for the input of the visco-plastic self-consistent model.

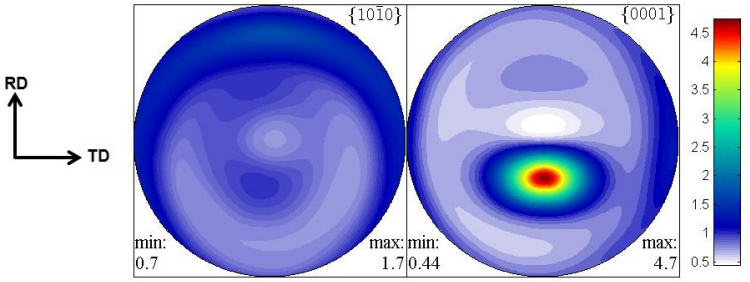

Fig. 1. (0001) and (1010) pole figures for the initial texture of the rolled Zinc alloy.

3. Modeling

In this section, the hardening model of Beyerlein and Tomé (2007) is briefly described. When a metallic material is reloaded after a certain amount of plastic prestrain, it usually exhibits significant changes in the reloading yield stress and hardening evolution depending on the mode and direction of reloading (Rauch et al., 2011; Barlat et al., 2013; Kitayama et al., 2013). Such a behavior can be affected by the texture anisotropy according to the reloading direction and the microstructure evolution in single crystals such as dislocation reversal-related mechanisms and cut-through phenomenon. In the model of Beyerlein and Tomé (2007), these mechanisms are accounted for and the CRSS is expressed as:

$$\Delta\tau_c^\alpha = \Delta\tau_h^\alpha + \Delta\tau_{cut}^\alpha + \Delta\tau_{rev}^\alpha \quad \text{where } \Delta\tau_{rev}^\alpha = \Delta\tau_B^\alpha + \Delta\tau_R^\alpha, \tag{1}$$

where $\Delta\tau_{cut}^\alpha$ is related to the effect of cut-through. $\Delta\tau_{rev}^\alpha$ represents the contribution of dislocation reversal-related mechanisms, which includes the contribution of the Bauschinger effect $\Delta\tau_B^\alpha$ and the extended reversal response $\Delta\tau_R^\alpha$. $\Delta\tau_h^\alpha$ represents the strength due to the dislocation accumulation/annihilation and patterning. This term can be calculated by the classic Voce law. In the Voce hardening law, the $\Delta\tau_h^\alpha$ for slip or twinning system s (contained on plane α) in a single crystal is calculated as follows:

$$\dot{\tau}_h^\alpha = \frac{\partial\tau_v^s}{\partial\Gamma} h^{\alpha\beta}\dot{\upsilon}^\beta \text{ with } \tau_v^s = \tau_0 + \left(\tau_1 + \theta_1\Gamma\right)\left(1 - \exp\left(-\Gamma\left|\frac{\theta_0}{\tau_1}\right|\right)\right), \tag{2}$$

wher Γ is the shear rate accumulated in each grain. The hardening parameters τ_0, τ_1, θ_0 and θ_1 can be determined by the experimental strain-stress curve. $h^{\alpha\beta}$ is the latent hardening coupling parameters which account for empirically the obstacles on system s ($s \in$ the plane α) associated with system s' ($s' \in \beta$). The detailed description of the Voce law can be found in Wang et al. (2013).

3.1. Cut-though effect

The cut-through mechanism is associated to the interaction between the slip systems newly activated during the strain path change and the non-coplanar obstacles generated during the pre-loading process. After a large pre-strain, some dislocation walls are created in single crystals which are commonly aligned with the slip planes which are relatively more active. When the strain path is suddenly changed, some slip systems that are non-coplanar to these obstacles will become active. In this case, the newly activated slip systems need to encounter an additional resistance when attempting to channel through these obstacles. In order to model this effect, a 'cut-through' matrix $X^{\alpha\beta}$ is proposed as follows:

$$X^{\alpha\beta} = \left\| \frac{\dot{\bar{\upsilon}}^{\alpha,n+1}}{\upsilon^\alpha} \times \frac{\bar{\upsilon}^\beta}{\upsilon} \right\| - \left\| \frac{\dot{\bar{\upsilon}}^{\alpha,n}}{\upsilon^\alpha} \times \frac{\bar{\upsilon}^\beta}{\upsilon} \right\| \qquad \alpha \neq \beta, \tag{3}$$

where $\dot{\bar{\upsilon}}^{\alpha,n+1}$ and $\dot{\bar{\upsilon}}^{\alpha,n}$ are the shear rates vectors in the plane α for the current and the previous strain increments. $\bar{\upsilon}$ represents the accumulated shear vector. υ^α is the normalized accumulated shear vector in plane α and υ refers to the sum of υ^α over all the slip planes

As shown by Eq. 83), the matrix $X^{\alpha\beta}$ accounts for the interaction between the slip systems in the plane α and the obstacles in the plane β considering the slip activity history. According to Beyerlein and Tomé (2007), if $X^{\alpha\beta} > 0$, an additional resistance to slips in plane α should be calculated. This resistance $\Delta\tau_{cut}^\alpha$ should be proportional to the 'strength' of the boundary τ_d which depends on the boundary characteristics like dislocation spacing d (Madec et al., 2002). After the reloading, the slip systems create channels gradually across the obstacles and the dislocation interspacing of the boundary β increases locally. Consequently, the strength needed to pass through the dislocations boundary β decreases gradually. $\Delta\tau_{cut}^\alpha$ is defined as a function of the accumulated shear on the plane α after reloading υ_{new}^α:

$$\Delta\tau_{cut}^\alpha = \tau_{cut,0}^\alpha \exp(-\omega\upsilon_{\text{new}}^\alpha) \text{ with } \tau_{cut,0}^\alpha = \sum_{\alpha\neq\beta} X_\alpha^\beta \tau_d^\beta, \tag{4}$$

where $\tau_{cut,0}^\alpha$ is the initial value of the cut-through strength. ω characterizes the rate at which newly activated systems dissolve the microstructure.

3.2. Bauschinger effect

During forward loading, a dislocation substructure is generated in the material, which induce internal stresses during pre-loading. Part of these internal stresses resists the applied loading and leads to the immobilization of dislocations during forward loading. During strain path change a fraction of the dislocations accumulated during forward loading glide in the reverse direction with low slip resistance and has a potential to recombine. This reversibility leads to a yield stress drop after reloading, which is usually known as Bauschinger effect (Bauschinger, 1881). To describe correctly the Bauschinger effect, an indicator $P^{\alpha\alpha}$ is introduced in this model to measure the reversibility of each slip system. The reversibility on the slip plane α is characterized by the sign and value of $P^{\alpha\alpha}$, which is defined as follows:

$$P^{\alpha\alpha} = \frac{\overline{\upsilon}^{\alpha}}{\upsilon} \cdot \frac{\dot{\overline{\upsilon}}^{\alpha}}{\dot{\upsilon}}, \quad -1 \le P^{\alpha\alpha} \le 1, \tag{5}$$

$P^{\alpha\alpha} \ge 0$ means that the shear on the plane α is not reversed while $P^{\alpha\alpha} = -1$ corresponds to full shear reversibility. In this case, the reverse shear can be calculated automatically during the simulation, which allows the prediction of the flow stress for multiple and arbitrary strain path changes. The evolution of $\Delta\tau_B^{\alpha}$ component with shear strain is captured by the following equation:

$$\Delta\tau_B^{\alpha} = \Delta\tau_{B,0}^{\alpha} \exp\left(-\frac{\upsilon_{new}^{\alpha}}{\upsilon_B}\right) \text{ with } \Delta\tau_{B,0}^{\alpha} = \mu P_0^{\alpha\alpha} \upsilon_{B,sat} \left(1 - \exp\left(-\vartheta_B \upsilon^{\alpha}\right)\right). \tag{6}$$

The parameter υ_B controls the rate at which the backstress effect appears with υ_{new}^{α}. $\Delta\tau_{B,0}^{\alpha}$ is the initial value at the instance of the strain path change, which depends on the reversibility through $P_0^{\alpha\alpha}$ (the value of $P^{\alpha\alpha}$ at the moment of reloading) and the dislocations ρ_B^{α} that are created on the slip plane α during the pre-strain. ρ_B^{α} is described by υ_{rev}^{α}, which evolves with the previously accumulated shear υ^{α} during the pre-strain. $\upsilon_{B,sat}$ is the maximum amount of shear that may be available, ϑ_B is the rate of saturation for reverse shear.

3.3. Extended reversal response

During the pre-loading, dislocations are locked in dislocation tangles and cell walls. After the reloading, some of the dislocations (ρ_R^{α}) get to slip more easily in the reverse. Unlike the Bauschinger effect, the dislocation density ρ_R^{α} can accumulate a large amount during the prestrain. A relatively large reverse strain is necessary for the release of these dislocations. The dislocations that are mildly locked require a small level of strain to be released while the others that more tightly locked need a higher reverse strain level. Therefore, an extended reversal response term $\Delta\tau_R^{\alpha}$ is introduced and defined as:

$$\Delta\tau_R^{\alpha} = \mu P_0^{\alpha\alpha} f'\left(\upsilon_{new}^{\alpha}\right). \tag{7}$$

The reversibility of the dislocations is described by the function $f(\upsilon) = \int_0^{\upsilon} f'(x)\,\mathrm{d}x$, which corresponds to the portion of ρ_R^{α} released by reverse shear υ. The evolution of $f'(\upsilon)$ is given by the empirical functions.

$$f' = f'_{peak} \frac{g}{g_{peak}} \text{ where } g = \exp\left(-\upsilon_{new}^{\alpha}/\upsilon_R\right) \text{lognormal}\left(\upsilon_{new}^{\alpha} \middle| \mu_R, \sigma_R\right), \tag{8}$$

where μ_R, σ_R and f'_{peak} are materials parameters, and υ_R is a measure of the pre-strain. A detailed description of this hardening model can be found in Beyerlein and Tomé (2007).

4. Result and discussion

The monotonic and reverse shear stress-shear strain curves for the Zn alloy sheet are simulated and compared with the experimental results (Fig. 2a). The simulation is carried out under full strain-imposed boundary condition. The best results are obtained using the secant interaction. It is worthy to note that the visco-plastic self-consistent model cannot capture the elasto-plastic transition. Therefore, to evaluate correctly the predicted curves, the elastic part of the experimental curves is removed from the results. The strain path change leads to a decrease of the yield stress after reloading and a variation the curve shape. The visco-plastic self-consistent framework associated with the new hardening law predicts successfully the deformation behavior. The values of the hardening parameters, listed in Table 1, are estimated by comparing the simulated and experimental responses under monotonic shear test along the rolling direction. The parameters associated with reverse loading are listed in Tabbe 2.

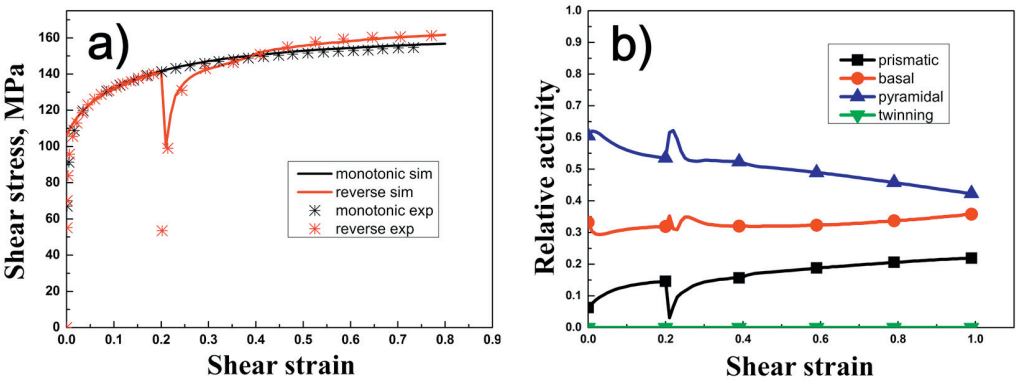

Fig. 2. (a) Predicted and experimental shear stress-shear strain curves for Zn alloy sheet in monotonic shear test and shear-reverse shear test; (b) Relative activities of the slip and twinning modes for shear-reverse shear test.

Table 1. Strain hardening parameters.

Secant model	τ_0 (MPa)	τ_1 (MPa)	θ_0 (MPa)	θ_1 (MPa)
Basal	7	5	130	5
Prismatic	180	41	90	4
Pyramidal	75	30	90	10
Twinning	400	0	0	0

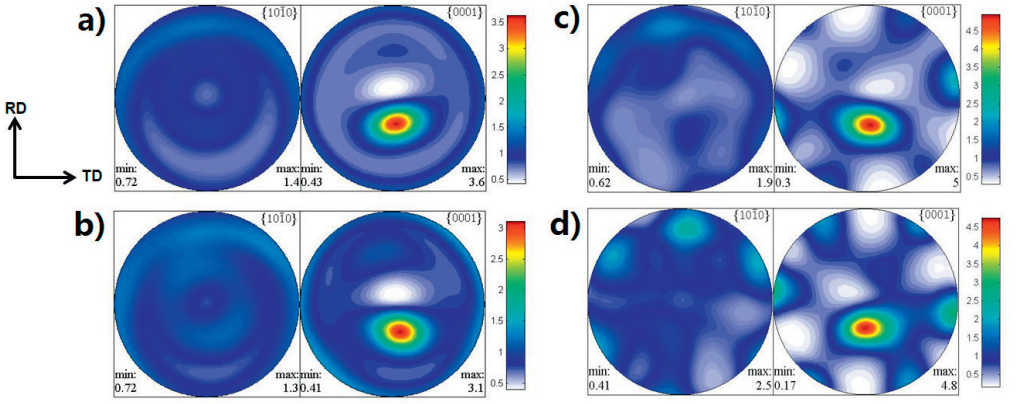

Fig. 3. (0001) and (1010) pole figures for: experimental texture after the pre-strain (a) and after reverse loading (b); predicted texture after the pre-strain (c) and after reverse loading (d).

The hardening parameters listed in Tab. 1 are in reasonable ranges according to previous studies (Fundenberger et al., 1997; Parisot et al., 2000). The variation with shear strain of relative activity for each deformation mode is shown in Fig. 2b. The simulations show that pyramidal slip accumulates most plastic deformation, followed by the basal and pyramidal slip systems. It is worth mentioning that, in these simulations, the activity of twinning is non-existent. The predicted texture evolution after pre-deformation and final deformation is shown in Fig. 3 and compared with experiments. Initially, the samples exhibits a texture with basal pole tilted at 20^o away from the normal direction toward the rolling direction (Fig. 1). After deformation, the tilted basal pole exists still. The predicted texture evolution is in good agreement with experimental results.

Table 2. List of the material-dependent parameters for zinc.

	Value
μ (shear modulus)	43GPa
μ_R (lognormal scale parameter)	0.25
σ_R (lognormal scale parameter)	0.85
θ_B (rate of saturation for reverse shear)	100
$\upsilon_{B,sat}$ (maximum shear available for Bauschinger effect)	0.012
υ_B (related to how fast the backstress is nullified)	0.025
υ_R (lognormal scale parameter)	0.12
f'_{peak} (material parameter)	0.0005
k_c (dislocation density coefficient)	0.03
X_C (empirical threshold value for the cut-through mechanism)	0.15
ω (rate of cut-through)	30
υ_1 (strain at which wall formation begins)	0.3
υ_2 (strain at which wall formation is completed)	0.7
k (a material-independent constant)	0.1

References

Agnew, S., Duygulu, O., 2005. Plastic anisotropy and the role of non-basal slip in magnesium alloy AZ31B, International Journal of Plasticity, 21 (6), 1161-1193.

Agnew, S.R., Yoo, M.H., Tomé, C.N., 2001. Application of texture simulation to understanding mechanical behavior of Mg and solid solution alloys containing Li or Y, Acta Materialia, 49, 4277-4289.

Barlat, F., Ha, J., Grácio, J.J., Lee, M.G., Rauch, E.F., Vincze, G., 2013. Extension of homogeneous anisotropic hardening model to cross-loading with latent effects. International Journal of Plasticity, 46, 130-142

Bauschinger, J., 1881. Ueber die VeraËnderung der Elasticita Ëtsgrenze und des ElasticitaËtsmoduls verschiedener Metalle. Civiling N.F. 27 (19), 289-348.

Beyerlein, I. J., Tomé, C.N., 2007. Modeling transients in the mechanical response of copper due to strain path changes, International Journal of Plasticity, 23, 640-664.

Kitayama, K., Tomé C.N., Rauch E.F., Gracio, J.J., Barlat, F., 2013. A crystallographic dislocation model for describing hardening of polycrystals during strain path changes. Application to low carbon steels, International Journal of Plasticity, 46, 54-69.

Lebensohn, R.A., Tomé, C.N., 1993. A self-consistent anisotropic approach for the simulation of plastic deformation and texture development of polycrystals: application to zirconium alloys, Acta Metallurgica et Materialia, 41, 2611-2624.

Madec, R., Devincre, B., Kubin, L.P., 2002. From dislocation junctions to forest hardening. Phys. Rev. Lett. 89, 255508-1-255508-4.

Molinari, A., Canova, G.R., Ahzi, S., 1987. A self-consistent approach of the large deformation polycrystal viscoplasticity. Acta Metallurgica, 35, 2983-2994.

Parisot, R., Forest, S., Gourgues, A.-F. , Pineau, A., Mareuse, D.,2000. Modeling the mechanical behavior of a multicrystalline zinc coating on a hot-dip galvanized steel sheet. Computational Materials Science, 19, 189-204

Proust, G., Tomé, C.N., Jain, A., Agnew, S.R., 2009. Modeling the effect of twinning and detwinning during strain-path changes of magnesium alloy AZ31. International Journal of Plasticity, 25, 861-880.322.

Rauch, E.F. 1998. Plastic anisotropy of sheet metals determined by simple shear tests. Materials Science and Engineering A, 241(1-2), 179-183.

Rauch, E.F., Gracio, J.J., Barlat, F., Vincze, G., 2011. Modelling the plastic behavior of metals under complex loading conditions. Modelling and Simulation in Materials Science and Engineering, 19, 1-18.